Eur Biophys J (2008) 37:483–493
DOI 10.1007/s00249-007-0240-5

ORIGINAL PAPER

Estimation of binding parameters for the protein–protein interaction using a site-directed spin labeling and EPR spectroscopy

Marcin Sarewicz · Sebastian Szytuła · Małgorzata Dutka · Artur Osyczka · Wojciech Froncisz

Received: 24 January 2007 / Revised: 25 October 2007 / Accepted: 28 October 2007 / Published online: 30 November 2007
© EBSA 2007

Abstract Sensitivity of the electron paramagnetic resonance (CW EPR) to molecular tumbling provides potential means for studying processes of molecular association. It uses spin-labeled macromolecules, whose CW EPR spectra may change upon binding to other macromolecules. When a spin-labeled molecule is mixed with its liganding partner, the EPR spectrum constitutes a linear combination of spectra of the bound and unbound ligand (as seen in our example of spin-labeled cytochrome c_2 interacting with cytochrome bc_1 complex). In principle, the fraction of each state can be extracted by the numerical decomposition of the spectrum; however, the accuracy of such decomposition may often be compromised by the lack of the spectrum of the fully bound ligand, imposed by the equilibrium nature of molecular association. To understand how this may affect the final estimation of the binding parameters, such as stoichiometry and affinity of the binding, a series of virtual titration experiments was conducted. Our non-linear regression analysis considered a case in which only a single class of binding sites exists, and a case in which classes of both specific and non-specific binding sites co-exist. The results indicate that in both models, the error due to the unknown admixture of the unbound ligand component in the EPR spectrum causes an overestimation of the bound fraction leading to the bias in the dissociation constant. At the same time, the stoichiometry of the binding remains relatively unaffected, which overall makes the decomposition of the EPR spectrum an attractive method for studying protein–protein interactions in equilibrium. Our theoretical treatment appears to be valid for any spectroscopic techniques dealing with overlapping spectra of free and bound component.

Keywords Site-directed spin labeling · Protein–protein association · Electron paramagnetic resonance · Ligand binding

M. Sarewicz · S. Szytuła · M. Dutka · A. Osyczka · W. Froncisz (✉)
Department of Biophysics, Faculty of Biochemistry, Biophysics and Biotechnology, Jagiellonian University, ul. Gronostajowa 7, 30-387 Kraków, Poland
e-mail: froncisz@mol.uj.edu.pl

Introduction

The process of ligand binding is one of the most important phenomena throughout biological systems, and its understanding lies within the scope of many research fields. The binding of low-molecular ligands, like hormones, ions or small peptides, can often be routinely measured using well-known methods including spectrophotometry (Green 1965), spectrofluorimetry (Yan and Marriott 2003) and isothermal titration calorimetry (ITC) (Leavitt and Freire 2001). Alternatively, surface plasmon resonance spectroscopy (Salamon et al. 1999; Salamon and Tollin 2001), flow cytometry (Stein et al. 2001) as well as radioactivity measurement of bound radioligands are sometimes used.

Investigations of macromolecular interactions are more difficult to perform, compared to studies on low-molecular ligands and can be directly measured, provided there exists a spectroscopic feature that changes upon binding. However, this is rarely the case (Erman and Vitello 1980) and requires applying fluorescence-labeled macromolecules (Yan and Marriott 2003) as well as the use of certain specific analytical methods. Indirect methods involving ITC do not require labeling of protein but encounter many restrictions due to buffer compositions, a large amount of high purity protein and special preparation of samples

(Doyle 1997; Pierce et al. 1999) to minimize baseline problems.

In electron paramagnetic resonance (EPR), site-directed spin labeling (SDSL) is often used to monitor structure and dynamics of proteins (Hubbell et al. 1998; Fajer 2000; Biswas et al. 2001; Columbus and Hubbell 2002). It relies on the introduction of paramagnetic nitroxide spin label compound (SL) to a selected site in the protein. Such spin label possesses the characteristic three-line EPR spectra, that are affected by several factors, including the molecular tumbling. SDSL could in principle be conveniently used to monitor the process of association of a labeled molecule with other molecules in solution. Indeed, EPR with spin-labeled lipids has proved to be a valuable method to study the interaction of lipids with proteins in biological membranes allowing determination of the lipid stoichiometry and the relative mean association constant (Marsh et al. 2002). The EPR spectroscopy was also used to investigate association of small spin-labeled peptides to a significantly larger protein molecule (Farahbakhsh et al. 1995) or membranes (Klug et al. 1995; Feix and Klug 1998).

Such studies encounter several methodological difficulties. One of them is the difficulty in the choice of the appropriate method of analysis. Data are typically analyzed using the Scatchard method (Scatchard 1949), which however appears not to be relevant for ligand binding analysis, especially for multi-class binding. This often obscures the interpretation of data (Norby et al. 1980; Munson and Rodbard 1983; Zierler 1989; Wang 1995; Wang and Jiang 1996). The situation becomes even more complicated when studying the association of two macromolecules (such as protein–protein interactions), in which case the data can often be described only qualitatively without extraction of any binding parameters (Park et al. 1997). This overall makes the EPR spectroscopy relatively seldom used for the study of ligand binding (Fajer 2000).

In this paper, we analyze the applicability of the EPR spectroscopy in studying protein–protein interactions in solution. We address the issue of the bias of the binding parameters due to the uncertainties in decomposition of the EPR spectrum. As those uncertainties mainly come from the lack of the spectrum of the fully bound ligand, imposed by the equilibrium nature of molecular association, we focus on the deconvolution of the EPR spectra of SL-protein mixed with its liganding partner and the examination of such deconvolution using a strictly analytical expression describing the binding isotherms under the ligand-depletion condition (Swillens 1995; Wang 1995; Wang and Jiang 1996). This allowed us to estimate the binding parameters such as the dissociation constant (K_d) and number of binding sites (n). The results show that the accuracy of these estimations is indeed compromised by the lack of the spectrum of the fully bound ligand resulting in the bias of the binding parameters K_d and n. We find, however, that the bias is only significantly present in a dissociation constant, whereas the number of binding sites usually remains relatively unaffected. This observation is discussed in the context of the potential applicability of the EPR spectroscopy for the study of protein–macromolecule interactions quantitatively.

Materials and methods

A numerical generation of pseudo-experimental data and a linear regression analysis was performed using Gnumeric 1.4.6. A multiple non-linear regression of three dimensional functions was carried out using Sigma Plot 8.0. For a symbolic transformation of the equations Maxima 5.6.1 was used.

Pseudo experimental data with randomly distributed errors were generated with a *randnorm* function built-in Gnumeric. A standard deviation of the spectrophotometric data, a limited accuracy of the syringe volume, and uncertainties of the linear regression decomposition of the EPR spectra were taken into account during the data generation. The values of relative standard deviations of the total protein concentration obtained from the spectrophotometric measurements were assumed to be in the range of 4% (for a typical assay). Relative standard deviations of the fraction values obtained from the linear regression analysis were assumed to be 2% (taken from the real EPR experiment). Accuracy of the titration volume was assumed to be 1% (Hamilton 2004). Theoretical EPR spectra were generated using the NLSL program (Budil et al. 1996) for the following values of magnetic and dynamic parameters: $g_{XX} = 2.0086$, $g_{YY} = 2.0066$, $g_{ZZ} = 2.0032$; $A_{XX} = 6.23$ G, $A_{YY} = 6.23$ G; $A_{ZZ} = 37$ G, $\tau_R = 0.4$ or 5 ns.

Single cysteine mutant cytochrome c_2 A101C from *Rhodobacter capsulatus* was isolated as decribed in Bartsh (1971) and labeled with MTSL spin label as described in Pyka et al. (2001). Cytochrome bc_1 complex was isolated using the procedure described in the literature (Robertson et al. 1993). A complex of cytochrome bc_1 with cytochrome c_2 was formed in 5 mM Tris buffer at pH 7.4, and 20 mM concentration of NaCl. Water was of an HPLC grade with 18.2 MΩ resistance. Tris and sodium chloride was purchased from Sigma Aldrich, and the MTSL spin label from Toronto Chemicals.

The CW-EPR spectra were recorded at room temperature on a locally constructed X-band spectrometer (Ilnicki et al. 1995), equipped with the rectangular loop-gap resonator using a quartz flat cell with a 0.4 mm by 4 mm cross-section (Piasecki et al. 1998). The following spectrometer settings were used: modulation amplitude 1 G, modulation

frequency 37 kHz, microwave power 0.86 mW, sweep with 100 G, time constant 10 ms, scan time 32 s, number of scans 25 or more.

Theory

Macromolecular association

The EPR spectrum of the mixture of the spin-labeled ligand with the binding macromolecule in solution will, in the simplest case consist of two overlapping components corresponding to the free and bound ligand. The shape of the EPR spectra of those two components depends on rates of rotational motion, expressed by the correlation time. Additionally, both spectra can be modified by the exchange between bound and free state of the spin-labeled ligand. The final resolution of the two distinct spectral components will depend on the exchange rate in relation to the time scale of the spin-label EPR spectroscopy. At X-band it is determined by the maximum anisotropy of the ^{14}N hyperfine splitting (A_{ZZ}–$A_{XX} \approx 10^8\ s^{-1}$). For the slow exchange rate, $\tau_{ex}^{-1} \ll 10^8\ s^{-1}$, the resulting spectrum will be represented by a linear combination of two EPR spectra that reflect different mobility of spin labels in the free and bound state of the ligand. When the exchange rate approaches the time scale of spin label EPR spectroscopy both spectra will be modified as is in case of the lipid–protein interface, which severely complicates analysis (Marsh and Horváth 1998). If the exchange frequency is equal or smaller than $2 \times 10^7\ s^{-1}$, the increase in peak-to-peak linewidth would not exceed 0.6 G. From the practical point of view, for the measurements done in the absence of other broadening factors, this is the upper limit for exchange frequency with broadening, which not yet influences the analysis. The initial investigation of the experimental spectra demonstrated lack of any line broadening of the composite spectra; therefore, assumption of slow exchange frequency was applied for further analysis.

Let us assume, that protein L (lately named ligand) with a spherical symmetry, having a radius r_1 = 7.3 Å is rigidly spin-labeled. According to the well known Stokes–Einstein–Debye formula:

$$\tau = 4\pi r^3 \eta / 3kT \quad (1)$$

In aqueous solution at 20°C, the rotational correlation time, τ_1 of such a ligand equals 400 ps. The simulated CW-EPR spectrum of such an isotropically rotating spin-labeled macromolecule is presented in Fig. 1a. After addition of the macromolecule P to the solution of a ligand L the association of these molecules will take place according to the following equation:

$$L + P <=> LP, \quad (2)$$

After association the spin label reports the motion of the whole LP complex. Assuming, as previously, that the LP complex possesses a spherical symmetry with radius r_2 equal to 19.3 Å, its rotational correlation time τ_2 increases to 5 ns. The simulated CW EPR spectrum of the complex is presented in Fig. 1b. The concentration of the complex [LP] will depend on the total concentration of the ligand [L], the total concentration of the binding macromolecule [P], the dissociation constant K_d and binding stoichiometry. An example of the simulated EPR spectrum for the 1:1 molar ratio of the bound and unbound state of the spin labeled protein is presented in Fig. 1c.

Decomposition of the CW EPR spectra into two components representing a bound and unbound state of SL-protein

Bound and free state of spin-labeled ligand spectrum is the linear combination of the "unbound" and "bound" spectrum according to the equation:

$$A(H) = cC(H) + fW(H), \quad (3)$$

where $C(H)$ and $W(H)$ are the EPR spectra of the SL-protein that is completely in either a bound or an unbound state, c and f are fractions of those component spectra in the spectrum $A(H)$. In order to estimate the parameters of this linear equation, a multiple linear regression procedure was used.

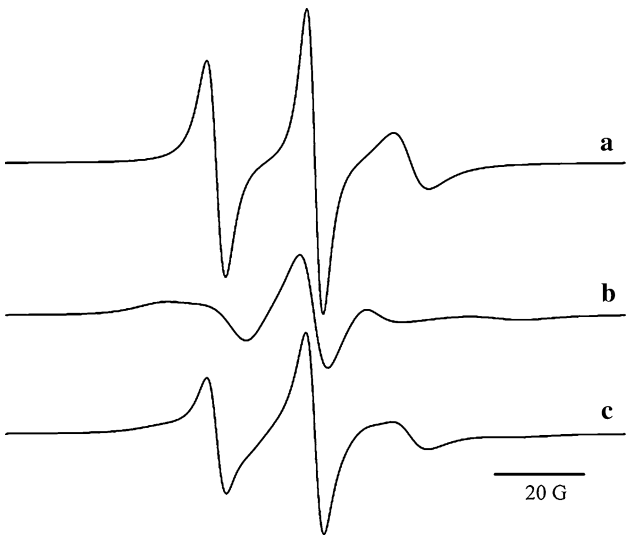

Fig. 1 Simulated one-component X-band CW-EPR spectra of a spin-labeled globular protein with radius 7.3 Å in water at 20°C. The spectrum corresponds to the free (**a**), fully bound (**b**) and half-bound (**c**) state of the protein. The half-bound spectrum represents the sum of spectrum (**a**) and (**b**) with the 1:1 intensity ratio

Let all the spectra be normalized against the spin concentration, thus:

$$c = 1 - f. \quad (4)$$

At an equilibrium the fraction of the unbound ligand is equal to f and the concentration of the bound ligand $[LP]$ is $(1-f)$ $[L]$. In order to obtain parameters c and f from the spectrum $A(H)$, one may choose a single feature of the CW-EPR spectrum, that changes upon binding (Park et al. 1997). However, in case of more complicated, multi-component spectra, it is difficult to decide which part of the spectrum is more sensitive to binding. Furthermore, the accuracy of such measurements is often very low, especially when changes are small and not linear. The method proposed in this study relies on multiple linear regression, that fits to the full set of data points in the experimental spectrum $A(H)$, the linear combination of full sets of data points from reference spectra $W(H)$ and $C(H)$. Using this method, the evaluation of corresponding fractions is based on the whole spectrum and not only on the arbitrary selected single point. At X-band rigid-limit spectra extends by about 80 G. When scan is digitized with 4,096 points/200 G, about 1,650 points describes the whole spin label spectra that are used for the linear deconvolution. As a result the estimation accuracy of c and f parameters is usually better than 2%.

In order to check the validity of the assumption of the slow exchange rate, the residual plot that represents the difference between the calculated and the experimental spectrum was examined for solutions that contain the SL-cytochrome c_2 and cytochrome bc_1 complex at various molar ratios. A representative experimentally obtained spectra are shown in Fig. 2. The reference spectra of free and bound cytochrome c_2 (Fig. 2a, b, respectively) were added with the calculated proportions giving *reconstructed* spectrum (Fig. 2c), that has identical shape to experimental spectrum measured in 1:1 molar ratio of cytochrome c_2/cytochrome bc_1 (Fig. 2d). Difference between *experimental* and *reconstructed* spectrum gives a residual plot representing just a noise with no noticeable trace of the EPR spectrum-like structure that would be observed for a faster exchange rate. A small bump that is seen in the center of the residual plot is presumably a result of limited accuracy of alignment of component spectra in the magnetic field. It is necessary to align the component spectra that are usually recorded for slightly different microwave frequencies before applying the linear regression procedure to the experimental spectra.

Difficulty in determination of the spectra of the bound state, C(H)

The spectrum of the spin-labeled ligand L in a free (unbound to the macromolecule) state $W(H)$, can be easily

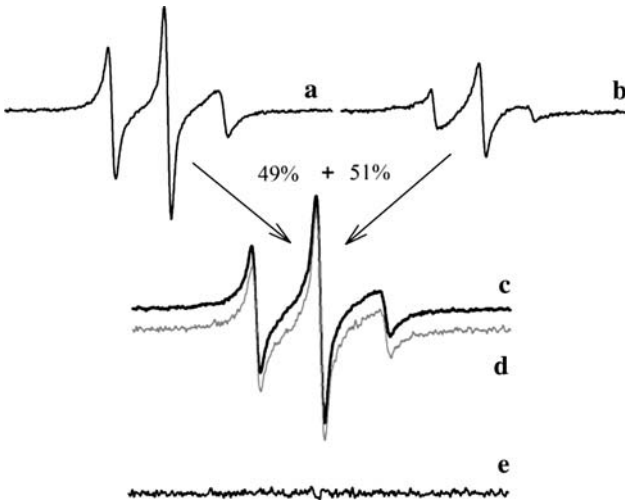

Fig. 2 Determination of the fraction of spin-labeled cytochrome c_2 that is bound to the bc_1 complex. Experimental EPR spectra of free (**a**) and bound (**b**) cytochrome c_2 that were added in proportions 49 and 51%, respectively, giving reconstructed spectrum (**c**) which is identical with experimental spectrum (**d**) recorded for the mixture of these two proteins in the 1:3 molar ratio. The difference (**e**) between the experimental and calculated EPR spectrum represents just a noise without any trace of a spectrum-like structure

registered in the absence of the binding protein P. There are, however, difficulties in obtaining the spectrum $C(H)$ that should be measured in conditions when $[P] >> K_d >> [L]$ due to limited sensitivity of the EPR spectroscopy and difficulties in obtaining a high concentration of the macromolecules. As a result the experimental spectrum, $C(H)$, is the sum of the component representing a fully bound ligand, $C^R(H)$, and some small unknown fraction, f^R, of a free component, $W(H)$. In some cases the spectral subtraction method can be used in order to obtain a spectrum that represents a fully bound ligand (Brotherus et al. 1980; Marsh 1989; Lewis and Thomas 1992; Marsh and Horváth 1998). This can be satisfactorily performed when the rotational mobility of the spin label in the bound state of the ligand is in the slow motional regime. In this case, the end point can be reached when the low-field line in the slow motion EPR spectrum is symmetrical as follows from the theory (Lewis and Thomas 1992). For the intermediate rotational motion of the spin label in the bound state of the ligand (typical situation for proteins labeled on the surface), it is difficult to accurately judge the end point of subtraction as observed in the present paper when studying an interaction of the cytochrome c_2 with the cytochrome bc_1 complex. As a consequence, the fraction of the bound state of the ligand is overestimated. This problem is analyzed quantitatively in the following sections.

In this case, the empirical reference spectrum $C(H)$ used for analysis is modified as follows:

$$c(H) = c^R C^R(H) + f^R\, W(H), \quad (5)$$

where: $C^R(H)$ is a spectrum of the totally bound ligand, c^R and f^R are fractions of spectra for the bound and free state of the ligand, respectively, in the spectrum C (H).

The substitution of Eqs. 4 and 5 into Eq. 3 gives the modified expression for $A(H)$ that takes into account the fact that the experimental reference spectrum for the bound state of the ligand contains a small, unknown admixture of the unbound ligand spectrum:

$$A(H) = c^R(1-f)C^R(H) + \left[(1-f)f^R + f\right]W(H). \quad (6)$$

The corrected fraction of the free ligand, r, is now equal to:

$$r = (1-f)f^R + f. \quad (7)$$

It is obvious, that in case when f^R is known, the analysis is reduced to the simple case of purely defined bound spectrum.

Analysis of the binding parameters from EPR data

The starting point for the EPR data analysis is classic equations describing binding curves. Present analysis was limited to two cases: binding to the single class of n independent sites with equal affinities (Model I) and the single class of n independent sites with equal affinities in the presence of a non-specific binding class (Model II).

In case of Model I the binding curve is described by the following equation (Stein et. Al. 2001):

$$[B] = n[P][F]/(K_d + [F]) \quad (8)$$

where: $[B]$—concentration of the bound ligand, $[F]$—concentration of the free ligand, n—the number of binding sites, $[P]$—the total concentration of binding macromolecules, K_d—a dissociation constant.

For the sake of the EPR sensitivity (a few micro moles per liter) measuring the concentration much lower than K_d ($[P] \ll K_d$) is possible only for weak interactions. Hence, during an experiment the large amount of ligand is in the bound state and the assumption that $[F] \approx [L]$ is no longer valid. Substituting $[F] = [L] - [B]$ into Eq. 8, after some rearrangements, the following analytical expression of the binding curve is obtained (Wang et al. 1992):

$$[B] = 0.5\left(K_d + [L] + n[P] - \sqrt{(K_d + [L] + n[P])^2 - 4n[P][L]}\right) \quad (9)$$

A fraction of the free ligand, r, is equal to:

$$r = [F]/[L] = 1 - [B]/[L], \quad (10)$$

Equating the right side of Eq. 10 to f that is calculated from the experimental EPR spectrum, one obtains an analytical relationship between the total concentrations of the ligand, $[L]$, the total concentration of the binding macromolecule, $[P]$, the dissociation constant K_d, and the number of binding sites n.

In case of two independent classes of binding sites, of which one has a much higher dissociation constant than the other, and for the ligand concentration $[F] \ll K_{d2}$, the low-affinity sites are apparently unsaturable, being a linear function of $[F]$ in the whole range of the total ligand concentrations used. Low affinity, non-specific bindings often come from impurities and/or binding of ligands to the lipid membranes. The Scatchard plots in the presence of such unsaturable class show non-linear curve with a horizontal asymptote. The binding curve, $[B']$ is equal to (Mendel and Mendel 1985; van Zoelen 1989):

$$[B'] = n[P][F]/(K_d + [F]) + \alpha[F] \quad (11)$$

where: α—the parameter describing a non-specific binding substitution $[F] = [L] - [B]$ into Eq. 11 gives after some rearrangements the quadratic equation of $[B']$. Its physically meaningful root is described by the following equation (Swillens 1995):

$$[B'] = 0.5a^{-1}\left(b - \left(b^2 - 4ac\right)^{0.5}\right) \quad (12)$$

where: $a = 1 + \alpha$;$b = -((K_d + [L])(1 + \alpha) + n[P] + \alpha[L])$; $c = [L](\alpha(K_d + [L]) + n[P])$.

The fraction of the unbound ligand is equal to:

$$r = [F]/[L] = 1 - [B']/[L], \quad (13)$$

Results and discussion

A typical EPR experiment on the macromolecular association involves progressive additions of small volumes of the concentrated SL-ligand into the EPR flat cell containing the binding macromolecule at the total concentration $[P]$. Successive additions of ligands make the macromolecule P more and more diluted due to the limited concentration of the stock solution of the SL-ligand. Therefore, it is impossible to maintain a concentration of macromolecule P within the 5% accuracy and at the same time to sufficiently cover the binding isotherm as advised by some authors (Wang and Jiang 1996). Thus the change of the total concentrations of both the ligand L and macromolecule P must be taken into account during the data analysis. This can be done using the analytical equations (Eqs. 8–13) presented earlier that depend simultaneously on both independent variables $[L]$ and $[P]$. In this case, the binding is described not by a curve in the two-dimensional plane but by a surface in the three-dimensional space. Binding parameters are obtained by fitting the relevant spatial functions to the experimental data using a non-linear three-dimensional regression. Each point on the binding surface

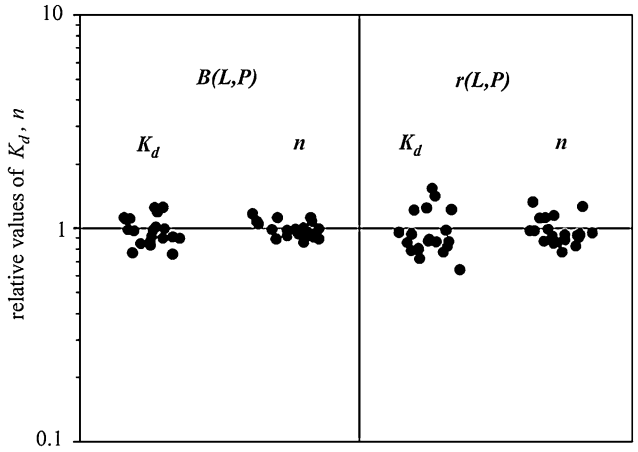

Fig. 3 Results of fitting to 20 independent computer generated titration experiments in case of the binding Model I. Estimated values of parameters: K_d^{est} (**a**) and n^{est} (**b**) are presented in relation to their true values. The parameters were obtained from fitting the analytical expressions, (Eqs. 9 and 10 describing a bound concentration, $B(L,P)$, and a fraction of the free ligand, $r(L,P)$ as a function of two independent variables L and P) to pseudo-experimental data

must fulfill, according to the appropriate model, the earlier equations (Eqs. 8–13).

In order to estimate the accuracy of that method, including the problem of the poorly defined end point of the spectral subtraction, 20 independent virtual experiments, mimicking the experimental titration, for both binding models were performed. The single pseudo-experimental series of data was generated using Eqs. 8 and 11 for Model I and Model II, respectively, to calculate proportions of free and bound ligand for given n, K_d and α. The errors from normally distributed population was calculated and added to each point separately. Then simulated spectra from Fig. 1 were mixed in calculated proportion and deconvoluted using spectrum for purely free, and bound ligand, contaminated with f^R admixture of the spectrum of free ligand. Binding parameters were obtained by fitting theoretical 3D binding surfaces to the computer-generated data points using appropriate analytic equation.

Model I of single class of n independent sites

Pseudo-data were generated using the following parameters: $n = 1$, $K_d = 50$ μM. Series of bound ligand concentrations, $[B]$, and fractions of unbound ligand, r, were obtained as a function of $[L]$ and $[P]$. These pseudo-data were fitted to corresponding equations (Eqs. 9, 10). As a result of fitting, 20 sets of K_d and n values for Eq. 9 together with 20 sets for Eq. 10 were obtained. A distribution of parameters estimated in such a way around their true values is presented in Fig. 3. Calculated relative values of binding parameters are grouped around 1, showing no bias in average dissociation constants and number of binding sites from true values. This suggests that the fitting of functions (Eqs. 9, 10) to the 3D data in respect to total concentrations of the ligand $[L]$ and binding macromolecule $[P]$ gives a reasonably good estimation without excessive values in standard deviations of the binding parameters (Table 1).

Table 1 Accuracy of binding parameters obtained from fitting an appropriate 3D binding function (Eqs. 9–10 and 12–13) to pseudo experimental data generated for two different models of binding sites

	Estimated value, X	Standard deviation of X: σ_X	Relative standard deviations: σ_X/X (%)
Model I (no non-specific bindings)			
From Eq. 9			
Number of binding sites n	0.99	0.09	9.1
Dissociation constant K_d	49.1	7.4	15.1
From Eq. 10			
Number of binding sites n	0.97	0.15	15.5
Dissociation constant K_d	48.0	12.0	25
Model II (with non-specific bindings)			
From Eq. 12			
Number of binding sites n	0.99	0.32	32.3
Dissociation constant K_d	52.5	22.0	41.9
Non-specific parameter α	0.448	0.015	3.4
From Eq. 13			
Number of binding sites n	1.05	0.27	25.7
Dissociation constant K_d	57.0	17.7	31.1
Non-specific parameter α	0.447	0.015	3.4

Data were generated using the following values of binding parameters: $n = 1$, $K_d = 50$ μM and $\alpha = 0.45$

Model II of single class of n independent binding sites in the presence of the non-specific binding

The same values of binding parameters, K_d and n, and $\alpha = 0.45$ were used to generate pseudo-data for this model. A series of bound ligand concentrations, $[B']$, and fractions of the unbound ligand, r, as functions of $[L]$ and $[P]$ were obtained. Pseudo-data points were fitted to corresponding equations (Eqs. 12, 13). As a result of fitting 20 sets of K_d , n and α values for Eq. 12 and 20 sets for Eq. 13 were obtained. The distribution of estimated parameters around their true values is presented in Fig. 4. The estimated values of all three binding parameters are again grouped around 1, showing no bias from their true values. This pseudo experiment suggests that fitting functions (Eqs. 12, 13) to the 3D pseudo-data in respect to the total ligand $[L]$ and binding macromolecule $[P]$ concentrations give reasonably good estimation of binding parameters without excessive values of their standard deviations for a chosen width of distribution of total concentrations of protein and ligand (Table 1).

In case of a single-class model without non-specific bindings, the average relative error of K_d and n estimation is lower by 10 and 6.3%, respectively, when fitting was performed using Eq. 9, in comparison with results of fitting to Eq. 10. For the binding model II that includes the presence of non-specific binding sites an absolute accuracy of K_d and n estimation is slightly lower than in model I. The average relative error of K_d and n estimation is larger by 10.4 and 6.4%, respectively, when fitting was performed using Eq. 12, in comparison with results of fitting to Eq. 13. However, in both cases, the true values of corresponding binding parameters lie within the uncertainty ranges of estimated values. This suggests that the three-dimensional analysis of experimental EPR data concerning the total concentration of the bound ligand $[B]$ obtained by multiplication of $(1-f)$ and $[L]$, as well as a fraction of the unbound ligand, r, directly from the linear regression, leads to the same results. In all cases, the accuracy of estimation of the K_d value is always lower than that for n.

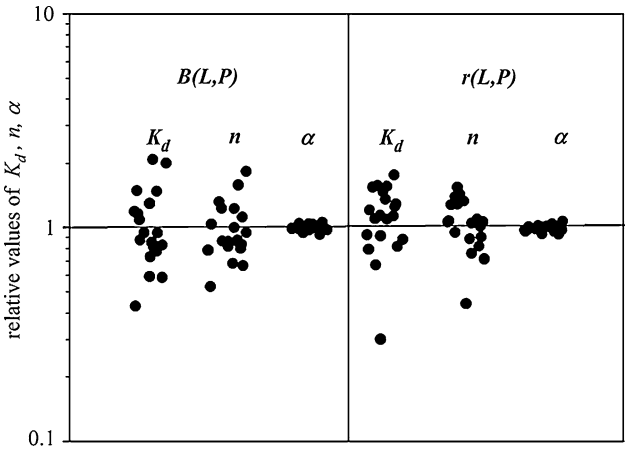

Fig. 4 Results of fitting to 20 independent computer generated titration experiments in case of the binding Model II that includes non-specific binding sites. Estimated values of binding parameters: K_d^{est} (**a**), n^{est} (**b**) and α^{est} (**c**) are presented in relation to their true values. The parameters were obtained from fitting of the analytical expressions, (Eqs. 12, 13) to pseudo-experimental data

Influence of the presence of the free ligand component in the reference spectrum that should represent a fully bound ligand on the precision of the binding parameters estimation

It is important to find out how the free component admixture, f^R, affects the accuracy of binding parameters estimations. For that purpose two sets of EPR spectra, corresponding to two investigated models of binding sites, were generated by linear combination (Eq. 3) of simulated reference spectra presented in Fig. 1a and b. Values of c and f that represent fractions of a bound and an unbound ligand were calculated according to both models. For each set of given values of binding parameters 20 pairs of c and f values were calculated each for a different value of the total ligand concentration in the range of 0 to 10 K_d keeping the protein concentration at the same level. This mimics the experimental titration procedure.

Theoretical spectra, $A(H)$, prepared according to the procedure described above were then decomposed by linear regression using two reference EPR spectra, $C(H)$ and $W(H)$. The first reference spectrum, $C(H)$, represented the bound ligand that was "contaminated" with a different amount, f^R, of the free ligand spectrum according to Eq. 5. The second reference EPR spectrum, $W(H)$, represented a purely unbound ligand.

The estimated values of fractions for the free and bound ligand, and corresponding values of $[B]$ and r, that are obtained in this virtual experiment are shifted from their true value to the extent that depends on the value of f^R. Fitting these estimated values to the corresponding analytical expressions of the binding curves (Eqs. 9, 12) gives distorted values of binding parameters.

Model I

In case of the single class of n independent binding sites an influence of f^R on estimation of binding parameters n and K_d was investigated for five different true values of dissociation constants (Fig. 5). The number of binding sites estimated for different values of f^R in the range of 0 and 0.4

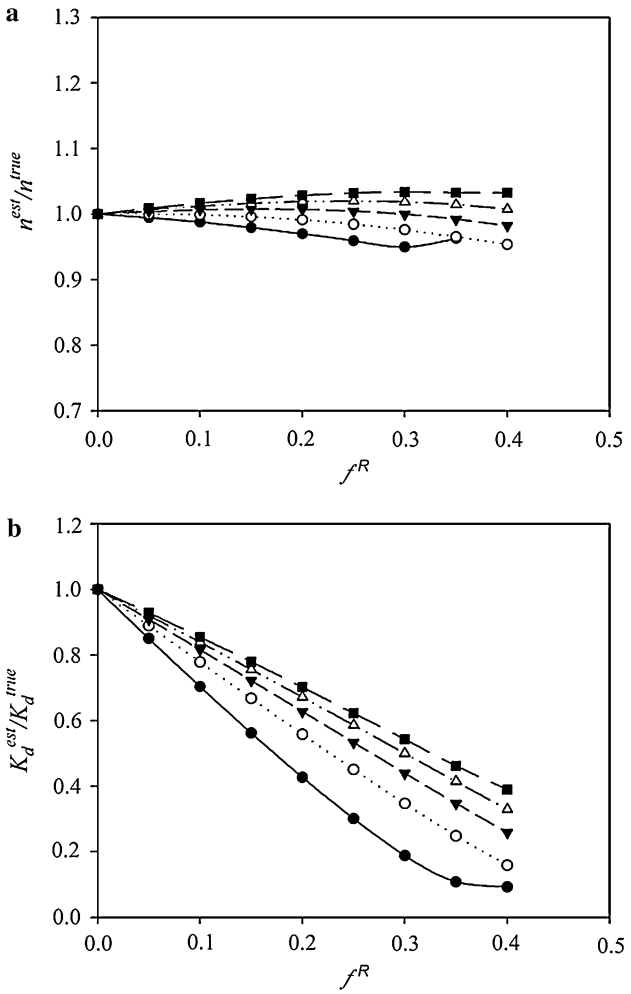

Fig. 5 Estimated values of the number of binding sites, n^{est} (**a**) and dissociation constant, K_d^{est} (**b**), normalized to their true values are plotted as a function of the fraction, f^R, of the unbound ligand EPR spectrum that contaminates the reference spectrum $C(H)$ (Eq. 5). Calculations were performed for the following values of the dissociation constant K_d^{true}: 30 μM (*filled circle*), 50 μM (*open circle*), 70 μM (*open circle*), 90 μM (*open triangle*) and 110 μM (*filled square*). The value of n was fixed at one and α at 0.5. The fittings were applied to the error-free data points generated with the use of Model I for binding sites

is virtually conserved. In the range of f^R and for 30 μM $< K_d <$ 110 μM apparent deviations of the estimated binding stoichiometry from its true values do not exceed 5% and are within the typical experimental uncertainty range. As one might expect for lower values of f^R deviations of calculated n from it true value are also smaller. Keeping this in mind, one may conclude that the difference between the estimated and the true value of n (Fig. 5a) is not bigger than the standard deviation of n that arises from scattered experimental values of protein and ligand concentrations used in the titration procedure. In contrast, the estimated values of the dissociation constant are significantly different from their true values for the investigated range of f^R. Successive increase of the free component admixture, f^R, in the reference spectrum $C(H)$ leads to a decrease of the estimated dissociation constant. This tendency is illustrated in Fig. 5b. It is evident that the rate of the decrease of that parameter with increase of f^R depends on its true value—the greater the binding affinity, the faster the decrease in the estimated dissociation constant. For f^R equals 0.2, the estimated values of dissociation constants are approximately within the 40% range (for K_d = 30 μM) to approx. 70% (for K_d = 110 μM) of their true values. In general, the estimated value of K_d is a direct function of the f^R parameter and an indirect function of the n parameter. Fortunately, as was concluded from the previous analysis the number of binding sites estimated from the EPR binding studies is almost independent of the value of the f^R parameter. This greatly simplifies the correction of the K_d parameter if the value of f^R can be estimated. Substituting Eq. 9 in 10 and equating that expression with Eq. 7, after rearrangements, the following equation for the true value of K_d is obtained:

$$K_d^{true}(f^R, f) = \left[f(1 - f^R) + f^R\right]\left(\frac{n[P]}{(f-1)(f^R-1)} - [L]\right) \quad (14)$$

Model II

In case of the single class of n independent sites with identical affinities in the presence of additional non-specific binding sites, there are three independent parameters describing the ligand binding: n, K_d and α in Eq. 11. Changes of the f^R value affect the values of all three binding parameters. For dissociation constants within the investigated range of 30–110 μM the number of binding sites is shifted less than 5% from its true value if $f^R < 0.25$ (Fig. 6a). For bigger values of f^R the estimated number of binding sites starts to deviate significantly from its true value especially for lower K_d values. Nevertheless, for the lower affinity of bindings the deviation of the calculated values of n from their true values does not exceed 10%. Apparent deviations of the estimated number of binding sites from its true values as a function of f^R, obtained for the dissociation constant K_d fixed at 50 μM and for various values of α are presented in Fig. 7. For investigated values of α and for $f^R < 0.25$ the calculated numbers of binding sites are virtually unchanged from their true values. In the range of f^R from 0.25 to 0.35 the calculated number of binding sites decreases by 10% from its true value, and above this level it starts to increase rapidly. It is seen from this plot that for f^R values between 0 and 0.3, an error of the n estimation does not exceed 5% of its true value. Deviations of estimated dissociation constants from their true values are dependent on f^R in a similar way as for the

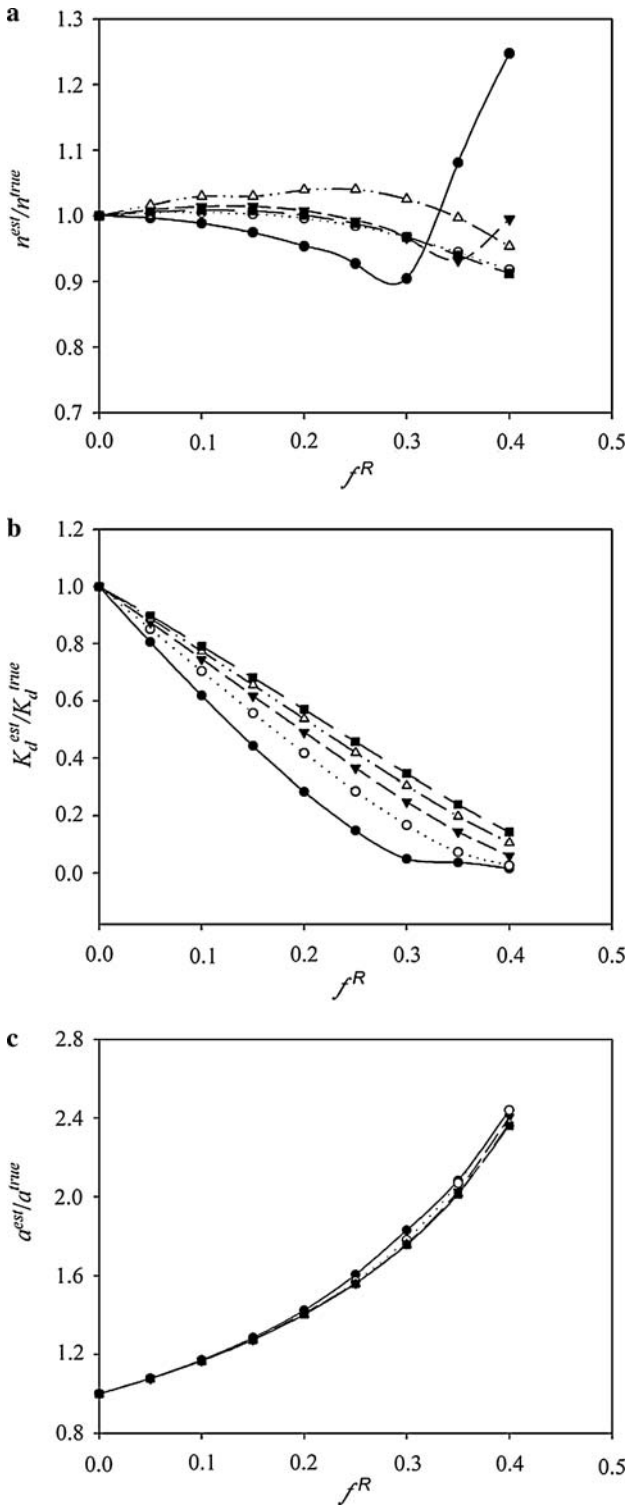

◀ **Fig. 6** Estimated values of the number of binding sites, n^{est} (**a**), dissociation constant K_d^{est} (**b**) and non-specificity parameter, α^{est} (**c**), normalized to their true values, plotted as a function of f^R. Calculations were performed for the following values of the dissociation constant K_d^{true}: 30 μM (*filled circle*), 50 μM (*open circle*), 70 μM (*open square*), 90 μM (*open triangle*) and 110 μM (*filled square*). The value of n was fixed at one and α at 0.5. The fitting was applied to the error-free data points generated using a single-class of binding sites model in the presence of non-specific binding—Model II

former model, but changes are more significant than previously. For the investigated dissociation constants and for $f^R = 0.2$ the obtained deviations of that parameter are within the range of approx. 40% (for $K_d = 30$ μM) to approx. 70% (for $K_d = 110$ μM) of their true values (Fig. 6b). The calculated value of the α parameter also depends on the value of f^R. It increases approximately exponentially with an increase of f^R. Relative deviations are significantly greater than for other parameters, and rapidly grow upon the α increase. When the free component fraction in $C(H)$ reaches 40% than the estimated value of α increases to 250% of its true value. For all investigated dissociation constants, the deviations of estimated values of the α binding parameter from their true values have very similar character (Fig. 6c). This suggests that the deviations of estimated α values from their true values are independent of the affinity of binding sites.

These observations indicate that, similarly to the previous model, the number of binding sites n estimated for $f^R < 0.35$ is very close to its true value. Due to the existence of three independent parameters, it is not possible to derive an algebraic function for the true value of K_d as was done for Model I of binding sites. In this case, there is only one equation that relates together all these parameters. Furthermore, an estimation of the true value of K_d requires the knowledge of its mathematical dependence on f and f^R assuming that the true values of n and α are known. Nevertheless, as the estimated relative values of α are nearly independent of K_d it follows from the inspection of Fig. 6c that parameter may be approximated by the semi-empirical exponential relation:

$$\alpha^{true}/\alpha = 1 + f^R \exp\left(\pi f^R\right). \tag{15}$$

This equation can be used to approximate the true value of α^{true} if the value of f^R can be estimated. Subsequently substituting Eqs. 12 in 13 and equating with Eq. 7, after some rearrangements, the following semi-empirical expression for the true values of the dissociation constant can be obtained:

$$K_d^{true}\left(f^R, f\right) = \left[f\left(1 - f^R\right) + f^R\right] \left(\frac{n[P]}{1 + (1 + \alpha^{true})[f(f^R - 1) - f^R]} - [L]\right). \tag{16}$$

In many cases, however, especially for the complicated multi-component spectra of the SL-protein, the estimation of f^R is not a trivial task. Fortunately, at least the maximal value of f^R can be evaluated from the spectral subtractions

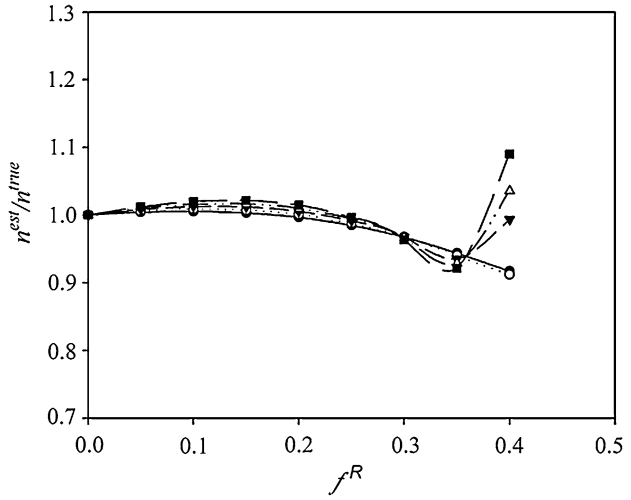

Fig. 7 Deviations of the estimated number of binding sites n^{est} from their true values as a function of f^R for different values of the parameter α (Eq. 11). Calculations are obtained for values of α equal to: 0.2 (*filled circle*), 0.3 (*open circle*), 0.4 (*open square*), 0.5 (*open triangle*) and 0.6 (*filled square*). The value of K_d^{true} was fixed at 50 μM and that of n^{true} at 1

and then, using Eq. 16, the range of true K_d values can be calculated. The simplest way to estimate f^R in the $C(H)$ spectrum is to successively subtract the fractions of the normalized reference $W(H)$ spectrum from the normalized $C(H)$ spectrum. When an excessive amount of $W(H)$ is subtracted, the resulting spectrum will be distorted and will no longer represent a realistic EPR spectrum of the immobilized spin label. Unacceptable spectral distortions define an upper limit for the spectral subtraction procedure allowing an estimation of the maximal value of the f^R parameter, what in turn gives the maximal range of uncertainties of the binding parameters. In consequence, one may use Eqs. 14 and 16 to reanalyze data in order to evaluate bias in estimated parameters without necessarily correcting every spectrum used for deconvolution.

Conclusions

Macromolecular association plays a crucial role in the functioning of many biological systems at the molecular level. This study shows that the use of the site-directed spin labeling and EPR spectroscopy to investigate the binding parameters of protein–protein interactions is very promising. There are many attractive features in this approach that are superior to other currently used methods. For example, the EPR measurements can be done in an opaque or dispersed media or in the presence of other macromolecules, which seemed to be essential for studying the effects of molecular crowding on the protein–protein associations (Ellis 2001a, b). Another attractive feature of the method is its high sensitivity such that only few picomoles of labeled proteins are required for a single titration point measurement.

The method is based on immobilization of the SL-protein upon binding to its partner. Thus, the accuracy of the method depends on the extent of spectral differences between the spectra of a bound and an unbound SL-protein. These differences can be enhanced by choosing the proper position of the SL attachment on the protein molecule for which the binding changes the spin label mobility in the most effective way. Alternatively, one may choose the microwave frequency for which the EPR spectra are the most sensitive to the change in SL mobility. Indeed, unpublished data revealed that similar changes in the SL mobility are significantly more reflected in the Q-band and W-band EPR experiments, at least in the case of the cytochrome c–bc_1 associations. This effect of the microwave frequency appears interesting for further analysis. Still another potential approach to differentiate the EPR spectra for the unbound and bound state of the spin-labeled ligand can be based on the different microwave saturation characteristics of those two states.

A general method of analysis of titration data in the EPR binding experiment is not different from a classical method of analysis used for the single class of binding sites. It can be easily extended to two independent classes of binding sites, with or without non-specific bindings, using the analytical methods described by Wang (1995). The accuracy of estimation of binding parameters is sensitive to many factors discussed earlier. So far, the major difficulties are related to the purity of the reference EPR spectrum that represents a fully bound SL-protein. Again, choosing a different microwave frequency may help to overcome or to minimize this problem.

We believe that the theoretical treatment presented in this work can be extended to any spectroscopic technique that deals with overlapping components representing a bound and free ligand.

Acknowledgment This work was supported by the State Committee for Scientific Research (KBN, Poland) grant KBN 3P04A 043 23.

References

Bartsh RG (1971) Cytochromes: bacterial. Methods Enzymol 23:344–363

Biswas R, Kuhne H, Brudvig GW, Gopalan V (2001) Use of EPR spectroscopy to study macromolecular structure and function. Sci Prog 84:45–67

Brotherus JR, Jost PC, Griffith H, Keana JF, Hokin LE (1980) Charge selectivity at the lipid–protein interface of membranous Na,K-ATPase. Proc Natl Acad Sci USA 77:272–276

Budil ED, Lee S, Saxena S, Freed JH (1996) Nonlinear-least-squares analysis of slow-motion epr spectra in one and two dimensions

using a modified Levenberg-Marquardt algorithm. J Magn Reson A 120:155–189
Columbus L, Hubbell WL (2002) A new spin on protein dynamics. Trends Biochem Sci 27:288–295
Doyle ML (1997) Characterization of binding interactions by isothermal titration calorimetry. Curr Opin Biotechnol 8:31–35
Ellis RJ (2001a) Macromolecular crowding: an important but neglected aspect of the intracellular environment. Curr Opin Struct Biol 11:114–119
Ellis RJ (2001b) Macromolecular crowding: obvious but underappreciated. Trends Biochem Sci 26:597–604
Erman JE, Vitello LB (1980) The binding of cytochrome *c* peroxidase and ferricytochrome *c*. A spectrophotometric determination of the equilibrium association constant as a function of ionic strength. J Biol Chem 10:6224–6227
Fajer PG (2000) EPR of proteins and peptides. In: Meyers RA (ed) Encyclopedia of analytical chemistry, Wiley, Chichester, pp 5725–5761
Farahbakhsh ZT, Huang QL, Ding LL, Altenbach C, Steinhoff HJ, Horwitz J, Hubbell WL (1995) Interaction of alpha-crystalin with spin-labeled peptides. Biochemistry 34:509–516
Feix J, Klug C (1998) Site-directed spin labeling of membrane proteins and peptide–membrane interaction. In: Berliner LJ (ed) Biological magnetic resonance, vol 14. Plenum, New York, pp 251–281
Green NM (1965) A spectrophotometric assay for avidin and biotin based on binding of dyes by avidin. Biochem J 94:23C–24C
Hamilton Syringe Calibration Report (2004)
Hubbell WL, Gross A, Langen R, Lietzow MA (1998) Recent advances in site-directed spin labeling of proteins. Curr Opin Struct Biol 8:649–656
Ilnicki J, Kozioł J, Oles T, Kostrzewa A, Galiński W, Gurbiel RJ, Froncisz W (1995) Saturation recovery EPR spectrometer. Mol Phys Rep 5:203–207
Klug CS, Su W, Liu J, Klebba PE, Feix JB (1995) Denaturant unfolding of the ferric enterobactin receptor and ligand-induced stabilization studied by site-directed spin labeling. Biochemistry 34:14230–14236
Leavitt S, Freire E (2001) Direct measurement of protein binding energetics by isothermal titration calorimetry. Curr Opin Struct Biol 11:560–566
Lewis LM, Thomas D (1992) Resolved conformational states of spin-labeled Ca-ATPase during the enzymatic cycle. Biochemistry 31:7381–7389
Marsh D (1989) Experimental methods in spin-label spectral analysis. In: Berliner LJ, Reuben J (eds) Biological magnetic resonance, vol 8. Plenum, New York, pp 255–303
Marsh D, Horváth LI (1998) Structure, dynamics and composition of the lipid–protein interface. Perspectives from spin-labeling. Biochim Biophys Acta 1376:267–296
Marsh D, Horváth LI, Swamy MJ, Mantripragada S, Kleinschmidt JH (2002) Interaction of membrane-spanning proteins with peripheral and lipid-anchored membrane proteins: perspectives from protein–lipid interactions (Review). Mol Membr Biol 19:247–255
Mendel CM, Mendel DB (1985) 'Non-specific' binding. The problem, and a solution. Biochem J 228:269–272
Munson PJ, Rodbard D (1983) Number of receptor sites from Scatchard and Klotz graphs: a constructive critique. Science 220:979–981
Norby JG, Ottolenghi P, Jensen J (1980) Scatchard plot: common misinterpretation of binding experiments. Anal Biochem 102:318–320
Park HY, Chun SB, Han S, Lee K, Kim K (1997) Interaction of cytochrome *c* and cytochrome *c* oxidase studied by spin-label EPR and site-directed mutagenesis. J Biochem Mol Biol 30:397–402
Piasecki W, Froncisz W, Hubbell WL (1998) A rectangular loop-gap resonator for EPR studies of aqueous samples. J Magn Reson 134:36–43
Pierce MM, Raman CS, Nall BT (1999) Isothermal titration calorimetry of protein–protein interactions. Methods 19:213–221
Pyka J, Osyczka A, Turyna B, Blicharski W, Froncisz W (2001) EPR studies of iso-1-cytochrome *c*: effect of temperature on two-component spectra of spin label attached to cysteine at position 102 and 47. Eur Biophys J 30:367–373
Robertson DE, Ding H, Chelminski PR, Slaughter C, Hsu J, Moomaw C, Tokito M, Daldal F, Dutton PL (1993) Hydroubiquinone-cytochrome *c2* oxidoreductase from *Rhodobacter capsulatus*: definition of a minimal, functional isolated preparation. Biochemistry 32:1310–1317
Salamon Z, Tollin G (2001) Plasmon resonance spectroscopy: probing molecular interactions at surfaces and interfaces. Spectrosc Int J 15:161–175
Salamon Z, Brown MI, Tollin G (1999) Plasmon resonance spectroscopy: probing molecular interactions within membranes. Trends Biochem Sci 24:213–219
Scatchard G (1949) The attractions of proteins for small molecules and ions. Ann NY Acad Sci 51:660–672
Stein RA, Wilkinson JC, Guyer CA, Staros JV (2001) An analytical approach to the measurement of equilibrium binding constants: application to EGF binding to EGF receptors in intact cells measured by flow cytometry. Biochemistry 40:6142–6154
Swillens S (1995) Interpretation of binding curves obtained with high receptor concentrations: practical aid for computer analysis. Mol Pharmacol 47:1197–1203
Wang ZX (1995) An exact mathematical expression for describing competitive binding of two different ligands to a protein molecule. FEBS Lett 360:111–114
Wang ZX, Jiang RF (1996) A novel two-site binding equation presented in terms of the total ligand concentration. FEBS Lett 392:245–249
Wang ZX, Kumar NR, Srivastava DK (1992) A novel spectroscopic titration method for determining the dissociation constant and stoichiometry of protein–ligand complex. Anal Biochem 206:376–381
Yan Y, Marriott G (2003) Analysis of protein interactions using fluorescence technologies. Curr Opin Chem Biol 7:635–640
Zierler K (1989) Misuse of nonlinear Scatchard plots. Trends Biochem Sci 14:314–317
van Zoelen EJJ (1989) Receptor–ligand interaction: a new method for determining binding parameters without a priori assumption on non-specific binding. Biochem J 262:549–556